JOC*Article*

Better Understanding of the Ring-Cleavage Process of Cyanocyclopropyl Anionic Derivatives. A Theoretical Study Based on the Electron Localization Function

Victor Polo,[†] Luis R. Domingo,*[,‡] and Juan Andrés*[,†]

Departament de Ciències Experimentals, Universitat Jaume I, Apartat 224, 12080, Castelló, Spain, and Instituto de Ciencia Molecular, Departamento de Química Orgánica, Universidad de Valencia, Dr. Moliner 50, 46100 Burjassot, Valencia, Spain

polo@sg.uji.es; andres@exp.uji.es

Received October 10, 2005

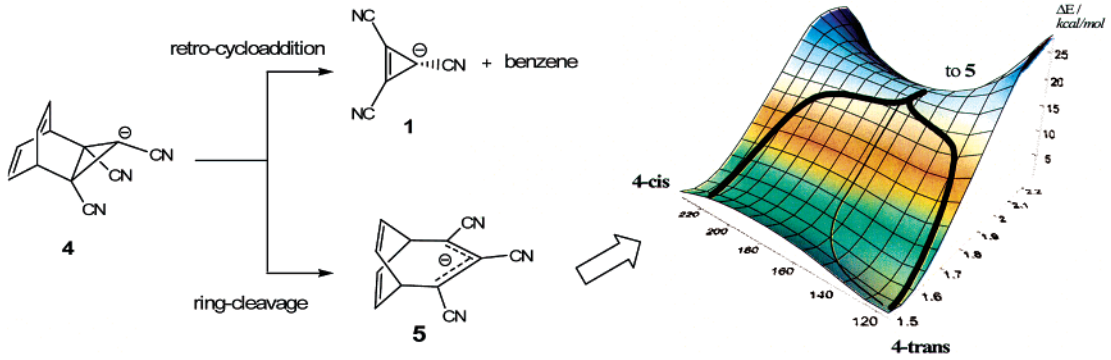

Theoretical calculations at the B3LYP/6-31+G(d), MP2/6-31+G(d), and G3(MP2) levels have been carried out to understand the alternative reaction pathways (the cyclopropyl ring cleavage (RC) and the retrocycloaddition reaction (rCA)) of a constrained tricyanocyclopropyl anionic derivative. The more energetically favorable path is found to be the RC process, a formally "forbidden" rearrangement (Leiviers, M.; Tam, I.; Groves, K.; Leung, D.; Xie, Y.; Breslow, R. *Org. Lett.* **2003**, *5*, 19, 3407) yielding an allylic anion system via a concerted transition structure, in agreement with experimental outcomes. rCA is more energetically favorable along a two-stage mechanism, via an intermediate, than a synchronous concerted process. By using isodesmic reactions, we have found that B3LYP presents limitations when it calculates carbon−carbon bond-breaking processes along the present rCA reaction. A detailed analysis of the nature of the topology of the reactive potential energy surface for the RC process points out the presence of a valley-ridge inflection point in the uphill part. An explanation for the low-energy barrier associated with RC is furnished on the analysis of the evolution of the twisting (dis-/conrotatory) motions of cyano substituents in the cyclopropyl ring as well as on the number and type of electron pairs provided by the electron localization function (ELF).

Introduction

Cyclopropane derivatives play a key role as useful building blocks in organic synthesis.[1] In particular, the release of a strain upon cycloaddition opens the way for subsequent chemical transformations. As part of these efforts, Breslow et al.[2] attempted to prepare the 1,2,3-tricyanopropenyl anion, **1**. They envisioned that the treatment of 1,2,3-tricyanochloropropenane with base to eliminate HCl and then deprotonate the resulting cyclopropene **2** should lead to **1**; however, apparently **2** undergoes anionic polymerization, and the synthesis of the anion

* To whom correspondence should be addressed. Phone: (+34) 964-728071. Fax: (+34) 964-728066 (J.A.).
[†] Universitat Jaume I.
[‡] Universidad de Valencia.

(1) (a) *Carbocyclic Three-Membered Ring Compounds. Methods of Organic Chemistry (Houben-Weyl)*; de Meijere, A., Ed.; Thieme: Thierne, Stuttgart, 1997; Vol. E17a−c. (b) Small Ring Compounds in Organic Synthesis I. *Top. Curr. Chem.*; de Meijere, A., Ed.; Springer: Berlin, Heidelberg, 1986; Vol. 133; 1987; Vol. 135; 1988; Vol. 144; 1990; Vol. 155; 1996; Vol. 178; 2000; Vol. 207. (c) *The Chemistry of the Cyclopropyl Group*; Rappoport, Z., Ed.; Wiley: Chichester, 1987. (d) Trost, B. M. In *Strain and its Implications in Organic Chemistry − Organic Stress and reactivity*; de Meijere, A., Blechert, S., Eds.; Kluwer Academic Publishers: Dordrecht, The Netherlands, 1989.

10.1021/jo052117h CCC: $33.50
Published on Web 12/22/2005

SCHEME 1

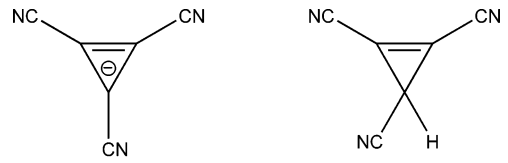

1 **2**

SCHEME 2

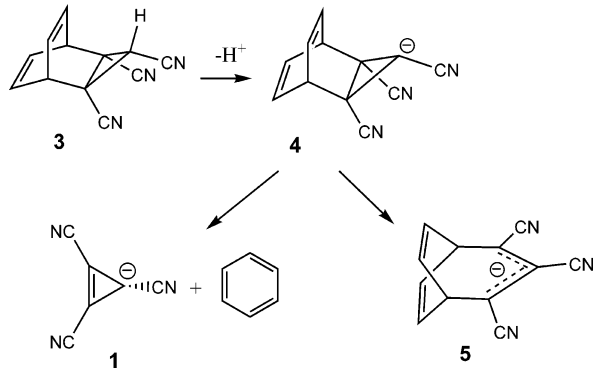

3 **4** **1** **5**

1 was unsuccessful[2] (see Scheme 1). Recently, these authors conceived an alternative plan in which the double bond of **1** would be introduced after negative charge was in place. Following this line of thinking, Breslow et al.[3] hoped that the deprotonation of **3** would yield its anion **4** (a barrelene system) and then fragment, via a retrocycloaddition (rCA) reaction, to form benzene and the anion **1**. The alternative ring cleavage (RC) to obtain **5** would not occur because it is a Woodward−Hoffmann (WH) forbidden process[4] along the disrotatory movement of the breaking cyclopropane σ-bond (C2−C3) at the anion **4** (see Scheme 2), and the allowed conrotatory motion would lead to a highly strained stereoisomer. However, contrary to these common assumptions, the formally forbidden rearrangement of **4** to **5** was found to be the principal process.[3]

To ascertain the results, theoretical considerations are needed, offering also an opportunity to connect computational studies to the experimental results reported by Breslow et al.[3] Recently, de Lera et al.[5] have characterized the transition structures (TSs) for the RC of cyclopropyl anion derivatives, emphasizing the substituent effects (−H, −CN, −Me) on the activation barrier, but the competitive rCA pathway was not considered. These authors[5] propose for structure **4**, on the basis of intrinsic reaction coordinate[6] (IRC) calculations, an initial conrotatory motion through a TS similar to that for the unconstrained system, but the direction of twisting changes to disrotatory further along the reaction path, to avoid a highly strained position of cyano groups by the fused rings.

The ring-cleavage reactions are interesting as well as challenging to study computationally because of the possibility of competitive pathways and the numerous aspects that can play a role in the reaction mechanism. Hence, throughout this work, the following issues will be considered: the study of the alternative rCA path; the suitable determination of the appropriate reaction coordinate to analyze the progress of the RC path; the role of cyano groups and the lone pair; the relationship among the height of the energy barrier, electronic rearrangements, and the direction of twisting along the RC rearrangement of **4**; and the stability of the allyl anion **5**. For these reasons, to understand and rationalize the experimental data, it is thus essential to map out the potential energy surface (PES) for a characterization of the corresponding stationary points and the reaction pathways connecting them and to carry out an investigation of the geometrical and electronic factors responsible for the unexpected low-energy barrier of the formally forbidden RC reaction in comparison with the rCA path.

The methods based on the topological analysis of the electron density or its Laplacian, such as atoms in molecules (AIM) of Bader[7] or the electron localization function (ELF) of Becke and Edgecombe[8] that was extensively developed by Silvi and Savin,[9] are well-suited approaches for the visualization of the electronic redistribution along a reaction pathway. The advantage of using the ELF methodology is that it provides a direct local measure of the Pauli principle, allowing a direct treatment of electron pairs and electronic delocalization and providing keys to understanding the roles played by the different chemical interactions. Several applications of the topological analysis for a better understanding of chemical bonding,[10] chemical reactivity,[11] and aromaticity[12] have been addressed recently.

The aim of the present contribution is to understand the reaction mechanisms that lead to the products via pathways that have the smallest activation energy; in particular, we would gain new insights on the reaction mechanism of the RC process of **4** and related systems. First, we provide theoretical support for the preference of the RC process instead of the rCA reaction. Second, a detailed ELF analysis of the reaction mechanism for the RC process is carried out to offer a sound rationalization of the underlying factors for the low activation barrier of this formally forbidden process and a rationalization of the successive changes in the direction of twisting of the cyclopropyl ring. For comparison purposes, two other related systems, the constrained 1-cyanocyclopropyl barrelene derivative (**6**) and

(2) Breslow, R.; Cortes, D. A.; Jaun, B.; Mitchell, R. D. *Tetrahedron Lett.* **1982**, *23*, 795.

(3) Leivers, M.; Tam, I.; Groves, K.; Leung, D.; Xie, Y. L.; Breslow, R. *Org. Lett.* **2003**, *5*, 3407.

(4) Woodward, R. B.; Hoffmann, R. *Angew. Chem., Int. Ed. Engl.* **1969**, *8*, 781.

(5) Faza, O. N.; Lopez, C. S.; Alvarez, R.; de Lera, A. R. *Org. Lett.* **2004**, *6*, 901.

(6) (a) Fukui, K. *Acc. Chem. Res.* **1981**, *14*, 363. (b) Gonzalez, C.; Schlegel, H. B. *J. Phys. Chem.* **1990**, *94*, 5523.

(7) (a) Bader, R. F. W. *Acc. Chem. Res.* **1985**, *18*, 9. (b) Bader, R. F. W. *Atoms in Molecules. A Quantum Theory*; Claredon Press: Oxford, 1990.

(8) Becke, A. D.; Edgecombe, K. E. *J. Chem. Phys.* **1990**, *92*, 5397.

(9) (a) Savin, A.; Becke, A. D.; Flad, J.; Nesper, R.; Preuss, H.; von Schnering, H. G. *Angew. Chem., Int. Ed. Engl.* **1991**, *30*, 409. (b) Silvi, B.; Savin, A. *Nature* **1994**, *371*, 683.

(10) (a) Llusar, R.; Beltrán, A.; Andrés, J.; Noury, S.; Silvi, B. *J. Comput. Chem.* **1999**, *20*, 1517. (b) Berski, S.; Latajka, Z.; Andrés, J. *Chem. Phys. Lett.* **2002**, *356*, 483. (c) Calatayud, M.; Berski, S.; Beltran, A.; Andres, J. *Theor. Chim. Acta* **2002**, *108*, 12. (d) Chamorro, E. *J. Chem. Phys.* **2003**, *118*, 8687. (e) Berski, S.; Gutsev, G. L.; Mochena, M.; Andrés, J. *J. Phys. Chem. A* **2004**, *108*, 6025. (f) Sambrano, J. R.; Gracia, L.; Andrés, J.; Berski, S.; Beltrán, A. *J. Phys. Chem. A* **2004**, *108*, 10850.

(11) (a) Berski, S.; Andrés, J.; Silvi, B.; Domingo, L. R. *J. Phys. Chem. A* **2003**, *107*, 6014. (b) Polo, V.; Andres, J.; Castillo, R.; Berski, S.; Silvi, B. *Chem.−Eur. J.* **2004**, *10*, 5165. (c) Michelini, M. D.; Russo, N.; Alikhani, M. E.; Silvi, B. *J. Comput. Chem.* **2005**, *26*, 1284. (d) Polo, V.; Andres, J. *J. Comput. Chem.* **2005**, *26*, 1427. (e) Cardenas, C.; Chamorro, E.; Notario, R. *J. Phys. Chem. A* **2005**, *109*, 4352. (f) Matito, E.; Sola, M.; Duran, M.; Poater, J. *J. Phys. Chem. B* **2005**, *109*, 7591.

(12) (a) Santos, J. C.; Andres, J.; Aizman, A.; Fuentealba, P. *J. Chem. Theory Comput.* **2005**, *1*, 83. (b) Santos, J. C.; Andres, J.; Aizman, A.; Fuentealba, P.; Polo, V. *J. Phys. Chem. A* **2005**, *109*, 3687. (c) Santos, J. C.; Polo, V.; Andres, J. *Chem. Phys. Lett.* **2005**, *406*, 393. (d) Poater, J.; Duran, M.; Sola, M.; Silvi, B. *Chem. Rev.* **2005**, *105*, in press.

1,2,3-tricyanocyclopropane (**8**), have been considered. In the next section, the computational methods and theoretical procedures are described. The main results and discussion are presented jointly in two subsections, accounting for an exploration of the PES and, in particular, the stationary points associated with both RC and rCA pathways and a more specific investigation on the reaction path of RC using the ELF method. Finally, the main conclusions that arise from the current research are summarized.

Theoretical Calculations

All calculations were carried out employing the GAUSSIAN03 program package.[13] All stationary points were optimized at the density functional theory (DFT) B3LYP/6-31+G(d)[14,15] and second-order perturbation theory MP2/6-31+G(d)[16] computing levels. All the bond-breaking processes are well described by the closed-shell formalism, and the converged wave function was stable with respect to a stability check.[17] For each optimized stationary point, a vibrational analysis was performed to determine its character, all positive for a minimum and one imaginary frequency for TS. Gibbs free energies were obtained at standard conditions of temperature (298.15 K) and pressure (1 atm).

Although Houk et al.[18] have shown that B3LYP is a suitable method for the study of pericyclic reactions, recent works by Radom et al.[19a] and Check and Gilbert[19b] point out some shortcomings of DFT calculations for the calculation of *relative* bond dissociation energies which can flaw the study of competitive reactions involving a different number of bond-breaking/-forming processes by DFT methods. To analyze this behavior, the stationary points of the two reaction pathways, RC and rCA, on PES were also optimized at the MP2/6-31+G(d) level. In addition, reliable calculations of reaction enthalpies for the RC and rCA channels were carried out by the highly accurate G3(MP2) procedure.[20] The G3(MP2) method predicts enthalpies of formation in the gas phase of organic molecules very close to experimental values.[21]

The ELF was defined as a measure of the local Pauli repulsion, and its topological analysis provides us with a useful and convenient partitioning of the molecular space into regions that are associated with chemically meaningful concepts such as atomic shells, bonds, and lone pairs. Each region, called a basin, is related to a local maximum (i.e., an attractor) of the ELF function, and it is interpreted as a region where it is more probable to localize an electron or a pair of electrons. The basins are either core basins labeled C(A) or valence basins V(A,...) belonging to the outermost shell. Valence basins are characterized by their coordination number (the synaptic order) with the core. Hence, lone pairs are represented by monosynaptic basins, covalent bonding between two atoms is represented by a disynaptic, and so on. This methodology has been well documented in a series of articles presenting its theoretical foundations.[9] A quantitative analysis is performed through the integration of the electronic density $\rho(\mathbf{r})$ in the volume of the ELF basin, Ω. The integrated basin population (N_i) of a given basin is calculated:

$$N_i = \int_{\Omega_i} \rho(\mathbf{r}) dr \quad (1)$$

Following the N_i along a calculated reaction path is a useful technique that allows identification of the specific flows of the electronic charge occurring along a chemical reaction and provides a rational characterization of chemical concepts, such as bond-forming/-breaking processes, obtaining new insights on the reaction mechanism. ELF analysis was carried out on the B3LYP/6-31+G(d) structures and was calculated along the RC reaction path using a cubical grid with a step size smaller than 0.1 bohr by the TopMod[22] package of programs.

TABLE 1. Relative[a] Energies (ΔE in kcal/mol) and Relative Free Gibbs Energies (ΔG in kcal/mol, Computed at 298 K) for the Stationary Points Involved in the Rearrangements of the Anion 4c[b]

	B3LYP		MP2	
	ΔE	ΔG	ΔE	ΔG
TSi	3.0	3.4	6.1	6.4
4t	0.1	0.4	0.7	1.0
TS1-I	18.3	17.4	20.1	19.2
5	−46.4	−45.5	−38.5	−39.2
TS1-II	11.9	10.1	13.9	12.0
IN-II	10.4	7.8	13.4	10.8
TS2-II	18.8	13.7	31.3	25.5
TS3-II	29.2	26.1	33.7	29.9
1 + benzene	3.4	−7.8	25.8	16.2

[a] Relative to **4c**. [b] All calculations were done using the 6-31+G(d) basis set.

Results and Discussion

Overview of the PES for the RC and rCA Processes of 4. First, it is necessary to indicate the presence of two conformers for the 1,2,3-tricyanocyclopropyl anion derivative (**4**) due to the two possible orientations, cis (**4c**) and trans (**4t**), of the C1−CN group with respect to the −CN groups located at the C2 and C3 carbon atoms. The cis conformer **4c** is 0.1 kcal/mol more stable than the trans one, **4t**, being the barrier for the interconversion of 3.0 kcal/mol via **TSi** (see Table 1); similar results were found by de Lera et al.[5]

An exhaustive exploration of the PES for the reactions of the tricyano derivative anion **4c** renders the presence of three reactive channels: one for the concerted RC process giving the allyl anion **5** (path RC in Figure 1) and two associated to the stepwise and concerted rCA reaction, yielding benzene and the desired cyclopropenyl anion **1** (path rCA in Figure 1). The following stationary points have been located and characterized: four TSs (**TS1-I**, **TS1-II**, **TS2-II**, and **TS3-II**), one intermediate (**IN-II**), and three possible products (**5** and **1** plus benzene). These stationary points along the three reactive channels have been depicted in Figure 1 together with the atom numbering, and the energetic results are listed in Table 1. The geometries of the TSs are plotted in Figure 2.

The values of free Gibbs activation energies associated with the RC, via **TS1-I**, are 17.4 (B3LYP) and 19.2 (MP2) kcal/mol. These energies are close to that obtained by de Lera et al.[5] (17.9 kcal/mol) for the RC of **4t** at the B3LYP/6-31++G-

(13) Gaussian 03, Revision C.02. See Supporting Information for a complete citation.
(14) (a) Becke, A. D. *J. Chem. Phys.* **1993**, *98*, 1372. (b) Becke, A. D. *J. Chem. Phys.* **1993**, *98*, 5648. (c) Lee, C. T.; Yang, W. T.; Parr, R. G. *Phys. Rev. B* **1988**, *37*, 785.
(15) Hariharan, P. C.; Pople, J. A. *Theor. Chim. Acta* **1973**, *28*, 213.
(16) Moller, C.; Plesset, M. S. *Phys. Rev.* **1934**, *46*, 618.
(17) Bauernschmitt, R.; Ahlrichs, R. *J. Chem. Phys.* **1996**, *104*, 9047.
(18) Guner, V.; Khuong, K. S.; Leach, A. G.; Lee, P. S.; Bartberger, M. D.; Houk, K. N. *J. Phys. Chem. A* **2003**, *107*, 11445.
(19) (a) Izgorodina, E. I.; Coote, M. L.; Radom, L. *J. Phys. Chem. A* **2005**, *109*, 7558. (b) Check, C. E.; Gilbert, T. M. *J. Org. Chem*., in press.
(20) Curtiss, L. A.; Redfern, P. C.; Raghavachari, K.; Rassolov, V.; Pople, J. A. *J. Chem. Phys.* **1999**, *110*, 4703.
(21) Notario, R.; Castaño, O.; Abboud, J. L. M.; Gomperts, R.; Frutos, L. M.; Palmeiro, R. *J. Org. Chem.* **1999**, *64*, 9011.
(22) Noury, S.; Krokidis, X.; Fuster, F.; Silvi, B. *Comput. Chem.* **1999**, *23*, 597.

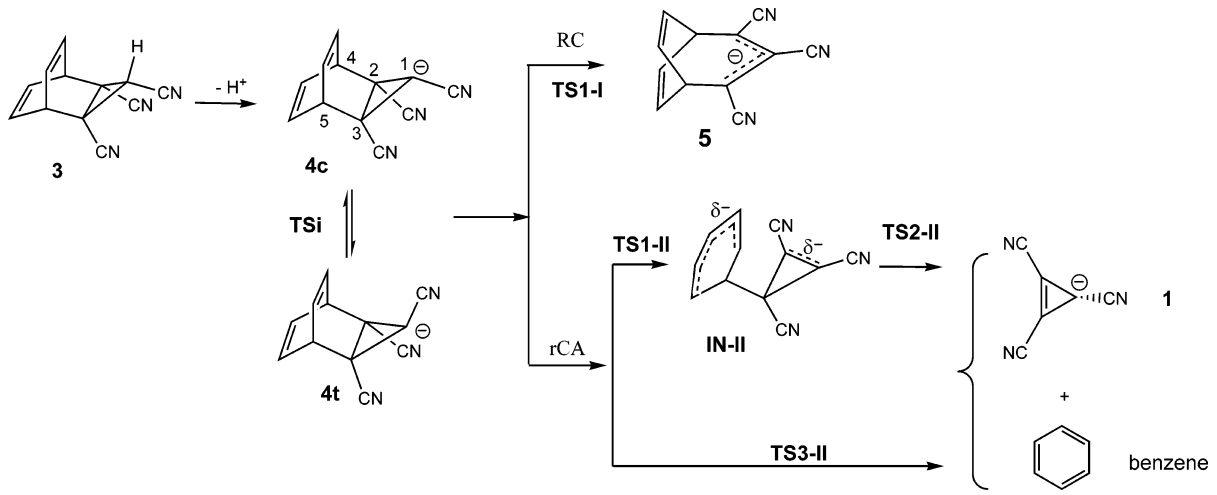

FIGURE 1. Schematic representation of species and reaction pathways studied in this work.

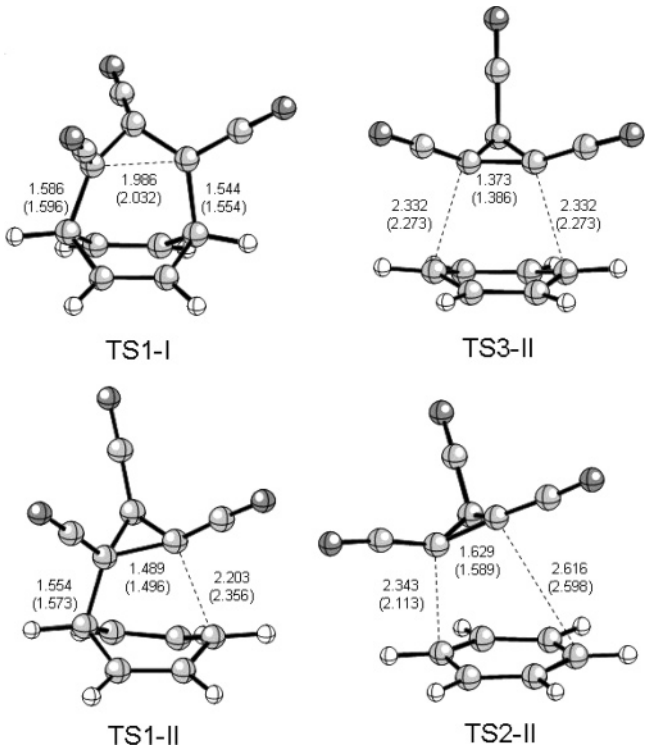

FIGURE 2. MP2/6-31+G(d) transition structures involved in the ring-cleavage process (in parentheses, B3LYP/6-31+G(d) results) of **TS1-I** and in the retrocycloaddition reaction: stepwise **TS1-II** and **TS2-II** and concerted **TS3-II** of anion **4**. Bond lengths are given in Å.

TABLE 2. Comparison of B3LYP/6-31+G(d), MP2/6-31+G(d), and G3(MP2) Calculated Reaction Enthalpies (in kcal/mol at 298 K) for the RC and rCA Pathways

	B3LYP	MP2	G3(MP2)
$\Delta_r H$(RC)	−45.1	−37.7	−39.1
$\Delta_r H$(rCA)	5.2	31.8	29.0

(d,p) level. Both B3LYP and MP2 predict this process as exergonic in 45.5 and 39.2 kcal/mol, respectively (see Table 2).

The stepwise and concerted pathways are found for the rCA reaction connecting the tricyano derivative anion **4c** to the products, **1** + benzene. For the stepwise rCA reaction, two TSs (**TS1-II** and **TS2-II**) and one intermediate (**IN-II**) have been found. The stepwise path is initialized by the C2−C4 breaking bond to give the intermediate **IN-II** via **TS1-II**. The increment of free energy associated with this bond-breaking process is 10.1 (B3LYP) and 12.0 (MP2) kcal/mol; the intermediate **IN-II** is located 7.8 (B3LYP) and 10.8 (MP2) kcal/mol above anion **4c**. An analysis of charges provided by the natural population analysis for **IN-II** shows that the negative charge is mainly located in the cyclohexadienyl moiety rather than in the tricyanocyclopropyl moiety. All attempts to find a biradical unrestricted broken-symmetry B3LYP solution for **IN-II** and **TS2-II** structures were unsuccessful, converging to the closed-shell solution. The barrier for the second step associated with the C3−C5 bond-breaking process, via **TS2-II**, is 3.6 (B3LYP) and 13.5 (MP2) kcal/mol above **TS1-II**. Therefore, this second step is the rate-limiting step of the stepwise rCA reaction. The concerted rCA process takes place by the simultaneous stretching and breaking of C2−C4 and C3−C5 bonds, being that the **TS3-II** is located 26.1 (B3LYP) and 29.9 (MP2) kcal/mol higher than the cycloadduct **4c**. It is worth noting that the rCA reaction follows a stepwise mechanism due to the presence of the anion and the cyano groups, in contrast to previous studies on unsubstitued related systems where the concerted mechanism was found to be the preferred one.[23]

B3LYP and MP2 calculations predict that the RC process of the anion **4** is strongly thermodynamically favored over the rCA path. However, B3LYP predicts that RC and rCA reactions are kinetically competitive processes, presenting similar values of free Gibbs energies for **TS1-I** and **TS2-II**, and MP2 shows that the RC process is the kinetically favorable process. In addition, there is a disagreement between the B3LYP and MP2 results for the reaction free energy of the rCA pathways: B3LYP predicts exergonic in 7.8 kcal/mol and MP2 yields endergonic in 16.2 kcal/mol. Thus, there is a substantial difference between the B3LYP and MP2 results, and this behavior increases as the reaction progresses along the rCA pathway. Comparing the values of B3LYP and MP2 with highly accurate G3(MP2) reaction enthalpies (see Table 2), the RC path presents a

(23) (a) Horn, B. A.; Herek, J. L.; Zewail, A. H. *J. Am. Chem. Soc.* **1996**, *118*, 8755. (b) Beno, B. R.; Wilsey, S.; Houk, K. N. *J. Am. Chem. Soc.* **1999**, *121*, 4816.

reasonable agreement of the three methods as to whether the rCA path is severely underestimated (~24 kcal/mol) by B3LYP.

It is important to recognize that finding the key issue to understanding the source of the difference between B3LYP and MP2 results is a difficult problem due to the complexity of **4** and the lack of available experimental data and external benchmarking. We have investigated different possibilities: (i) calculated values of aromatization energies of **1**, (ii) calculation of the ring strain of **4c** using homodesmic reactions,[24] and (iii) calculation of isodesmic bond separation reactions. For (i) and (ii), the results obtained at both B3LYP and MP2 levels were similar. However, substantial differences were observed in the calculation of (iii).[25] The same discrepancies are also found in related systems containing a bicyclo[2.2.2]oct-2,5-diene moiety. In this sense, further insight can be gained by calculation of the following isodesmic reaction 2 for a direct estimation of the bond dissociation energies of breaking of the C2−C4 and C3−C5 bonds without reorganization of the involved electron pairs:

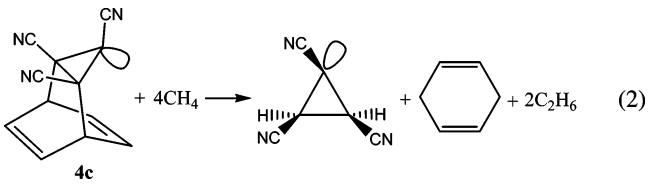

(2)

The values for the reaction energy of reaction 2 (E(**4c**) + 4E(CH_4) − E(tricyanocyclopropyl anion) − E(1,4-hexadiene) − 2E(C_2H_6)) are 10.9, −10.8, and −9.9 kcal/mol calculated at the B3LYP/6-31+G(d), MP2/6-31+G(d), and G3(MP2) levels, respectively. Thus, a discrepancy of the same magnitude as that observed in the rCA path of **4c** is shown in reaction 2 suggesting an understabilization of **4c** with respect to the products by the B3LYP method. B3LYP falls when it calculates bond dissociation energies associated to carbon−carbon bond-breaking processes, C2−C4 and C3−C5, along the rCA reaction. Very recently, an underestimation of the C−C bond energy B3LYP has been adressed.[19b] For a [2+2] cyclization between tetramethylethene and various alkenes where two C−C bonds are formed/broken similarly to our rCA pathway, errors up to 25.3 kcal/mol (compared to G3(MP2) results) have been reported.[19b] However, along the RC path, C2−C4 and C3−C5 bonds are preserved and similar values are found for the activation and reaction energies at B3LYP and MP2 computing levels.

Analysis of the geometrical parameters indicates that both computational levels, B3LYP and MP2, present a large equilibrium distance (1.60 and 1.58 Å) for the C2−C4 and C3−C5 bond lengths at **4c**, respectively. In a previous work by Birney et al.[26] on the rCA for related structures containing the bicyclo-[2.2.1]octene moiety, the large C−C distance is justified by means of a molecular orbital analysis. In our case, there is a double interaction of π occupied orbitals of the C−C double bonds with the σ* virtual orbitals of C2−C4 and C3−C5 bonds in the cycloadduct **4c**. These interactions lengthen and weaken these bonds, and this behavior is nicely related to the high reactivity of **4c**. Similar B3LYP and MP2 geometrical results are found for the breaking bonds in **TS1-I** (rC2−C3 = 2.03 (B3LYP) and 1.99 Å (MP2)), and an earlier **TS1-II** is predicted by MP2 (rC2−C4 = 2.35 (B3LYP) and 2.20 Å (MP2)). At the intermediate **IN-II**, the distance between the C2 and C4 centers is 2.45 (B3LYP) and 2.55 Å (MP2), indicating that the bond is already broken, and the C3−C5 bond remains at 1.58 (B3LYP) and 1.55 Å (MP2). B3LYP calculation of **TS2-II** gives an earlier structure than MP2, with the length of the C3−C5 breaking bond of 2.11 (B3LYP) and 2.34 Å (MP2). The synchronous concerted **TS3-II** gives similar lengths for C2−C4 and C3−C5 breaking bonds at the B3LYP and MP2 levels of 2.27 and 2.33 Å, respectively.

The analysis of the atomic motion at the unique imaginary frequency of **TS1-I**, 280.3i (B3LYP) and 352.9i (MP2) cm^{-1}, indicates that this TS is mainly associated with the displacement of the C2 and C3 atoms along the C2−C3 breaking bond, and the movement of the two cyano groups present on the C2 and C3 atoms is negligible. For **TS1-II**, the imaginary frequency, 155.1i (B3LYP) and 226.0i (MP2) cm^{-1}, is associated with the displacement of the C2 and C4 atoms along the C2−C4 breaking bond. Finally, the imaginary frequency of **TS2-II**, 301.0i (B3LYP) and 226.0i (MP2) cm^{-1}, is related to the C3−C5 breaking-bond process. Because of the symmetry of the system, the concerted rCA pathway lies between the two degenerate stepwise processes, and the corresponding **TS3-II** presents two imaginary frequencies: one, 366.4i (B3LYP) and 276.4i (MP2) cm^{-1}, is associated with the simultaneous stretching of the C2−C4 and C3−C5 bonds, and the other, 320.8i (B3LYP) and 164.0i cm^{-1} (MP2), is associated with the formation of C2−C4 and the breaking of C3−C5 and vice versa.

Finally, a note of caution is mandatory. Recent studies have warned about an overestimation of the correlation energy by DFT methods[27] for TSs of similar nature and have recommended the use of multiconfigurational approaches including dynamical correlation effects (for instance, the CASPT2 method) on top of the B3LYP optimized geometries. Unfortunately, the present article explores two distinct pathways (RC and rCA) involving different bond-breaking/-forming processes that would require a very large active space for a balanced coverage of the correlation energy that exceeds the actual computational capabilities. More extensive calculations will be required, however, to pin down accurate results for the rCA reaction mechanism.

Why Does the Direction of the Twisting Motion Change along the RC Process of 4c−t? An Explanation Based on the ELF analysis. For a further investigation of how this forbidden RC rearrangement occurs, an examination of the PES projected into the rC2−C3 distance and the dihedral angle dC10−1−2−3 as selected geometrical variables (see Figure 3) provides some clues on the convenient choice of the reaction path. The uphill part of the PES presents a valley-ridge inflection point (VRI)[28] located along the reaction path connecting **TSi** associated with the inversion of a lone pair on C1 and **TS1-I**; this type of event on PES has been recently classified as the

(24) Khoury, P. R.; Goddard, J. D.; Tam, W. *Tetrahedron* **2004**, *60*, 8103.
(25) Hehre, W. J.; Radom, L.; Schleyer, R. v. R.; Pople, J. A. *Ab Initio Molecular Orbital Theory*; Wiley: New York, 1986.
(26) (a) Pool, B. R.; White, J. M. *Org. Lett.* **2000**, *2*, 3505. (b) Birney, D.; Lim, T. K.; Koh, J. H. P.; Pool, B. R.; White, J. M. *J. Am. Chem. Soc.* **2002**, *124*, 5091.
(27) Khuong, K. S.; Houk, K. N. *J. Am. Chem. Soc.* **2003**, *125*, 14867.
(28) One of the earliest discussions of valleys and ridges on potential energy surfaces: (a) Metiu, H.; Ross, J.; Silbey, R.; George, T. F. *J. Chem. Phys.* **1974**, *61*, 3200. The valley-ridge inflection point has been extensively discussed by Ruedenberg et al. (b) Valtazanos, P.; Elbert, S. T.; Ruedenberg, K. *J. Am. Chem. Soc.* **1986**, *108*, 3147. (c) Valtazanos, P.; Ruedenberg, K. *Theor. Chim. Acta* **1986**, *69*, 281. (d) Basilevsky, M. V. *Theor. Chim. Acta* **1987**, *72*, 63. (e) Baker, J.; Gill, P. M. W. *J. Comput. Chem.* **1988**, *9*, 465. (f) Andres, J.; Cardenas, R.; Silla, E.; Tapia, O. *J. Am. Chem. Soc.* **1988**, *110*, 666. (g) Tapia, O.; Lluch, J. M.; Cardenas, R.; Andres, J. *J. Am. Chem. Soc.* **1989**, *111*, 829.

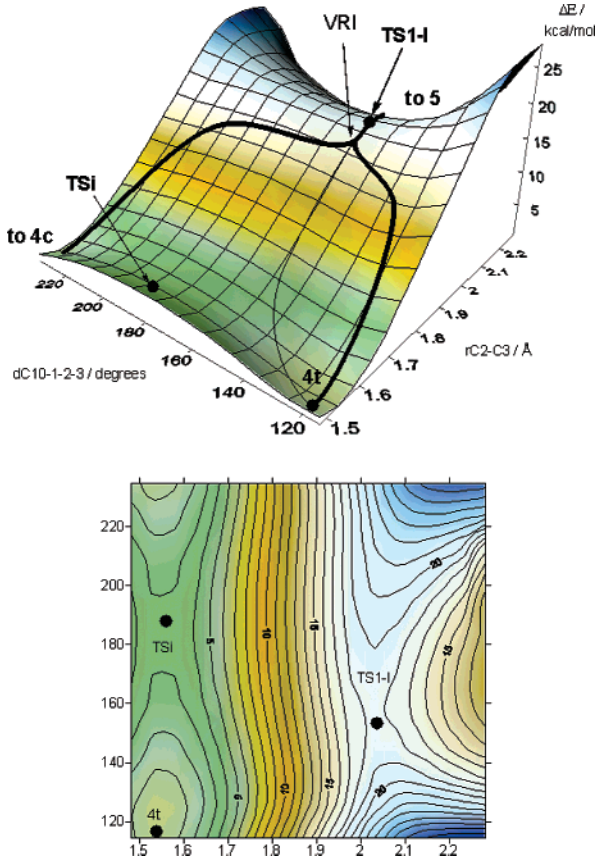

FIGURE 3. Three- and two-dimensional projections of the potential energy surface for the ring cleavage of tricyanocyclopropyl anionic derivative **4c**−**t** to **5**. The energy relative to **4c** is plotted with B3LYP/6-31+G(d)-constrained, optimized structures at intervals of 0.05 Å, rC2−C3 distance, and of 10°, dC10−1−2−3 dihedral angle. Stationary points are located by circles: **4c** (1.53, 245.1), **TSi** (1.55, 184.5) and **TS1-I** (2.03, 154.6), **4t** (1.53, 116.1), and **5** (2.52, 180.0) lie outside the surface. The reaction paths traced by the IRC (plane line) and the rC2−C3 driving coordinate from **4c** and **4t** (bold lines) are depicted on the three-dimensional surface together with the valley-ridge inflection point (VRI).

uphill bifurcating ridge by Quapp.[29] A number of chemical reactions present similar topologies, in which one TS connects directly to another TS via a VRI, which have been reported in the literature.[30] An analysis of Figure 3 shows that two valleys appear on the reactant side, **4c** and **4t**, and only one appears on the product side, **5**. The calculation of the IRC is a good model for the reaction path if the TS is connected to the minimum by a continuous valley (convex isopotential hypersurface). However, the presence of the VRI makes the IRC procedure not a

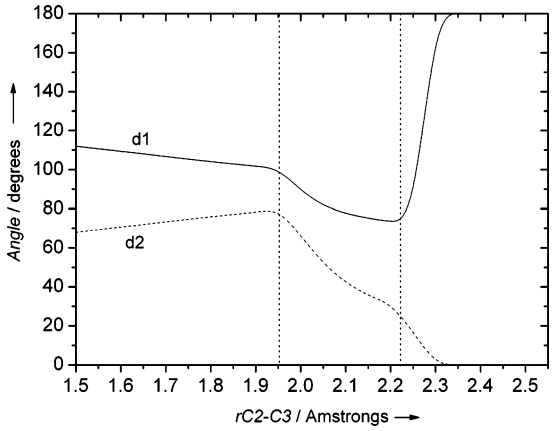

FIGURE 4. Dependence of dihedral angles d1 and d2 (as defined in Scheme 3) with respect to the reaction path traced by the distinguished rC2−C3 coordinate from **4t** to **5** (**TS1-I** located at 2.03 Å). Vertical lines mark the change of the twisting motion (dis-/con-/disrotatory).

SCHEME 3. Definition of Dihedral Angles d1, d2, and d3

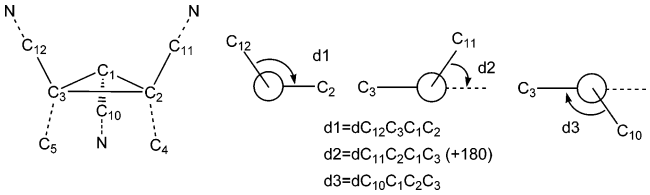

suitable model for this reaction path (see Figure 3, plain line), as it has been remarked by Quapp[29] for similar topologies. An appropriate approach to overcome this limitation is the use of a driving coordinate along the "reaction valley" of the minimum, performing an energy optimization for the remaining coordinates. Although modern implementations of this method have been recently developed,[31,32] inspection of Figure 3 shows that a reasonable reaction path can be obtained by selecting the rC2−C3 distance, associated with the bond-breaking process, as the driving coordinate (Figure 3, bold lines). As we have discussed previously, the choice of the **4c**−**t** is chemically irrelevant, and we considered the reaction path from **4t** because it presents a lower-energy reaction path than the one of **4c**.[33] This use of a driving coordinate to trace the reaction path presents the problem, among others,[34] that the step size is not fixed, and relevant geometrical changes involving other parameters may be overlooked. Closer inspection of the calculated path reveals that, for rC2−C3 values between 2.30 and 2.35 Å, the conformation of the cyano group at the C2 atom changes suddenly, leading to a large stabilization of the system.

Along the calculated reaction path, the twisting direction of the cyclopropyl group is monitored by means of the relative motion of the cyano groups C2−CN and C3−CN with respect to the plane determined by the C1−C2−C3 atoms (see Figure 4; a definition of dihedral angles d1 and d2 is given in Scheme 3), and the integration of the density charge over the ELF basins (see Figure 5) accounts for the rearrangements of the electronic structure (see Scheme 4).

(29) Quapp, W. *J. Mol. Struct.* **2004**, *695*, 95.
(30) More recent discussions and applications include: (a) Yanai, T.; Taketsugu, T.; Hirao, K. *J. Chem. Phys.* **1997**, *107*, 1137. (b) Kumeda, Y.; Taketsugu, T. *J. Chem. Phys.* **2000**, *113*, 477. (c) Ramquet, M. N.; Dive, G.; Dehareng, D. *J. Chem. Phys.* **2000**, *112*, 4923. (d) Castano, O.; Frutos, L. M.; Palmeiro, R.; Notario, R.; Andres, J. L.; Gomperts, R.; Blancafort, L.; Robb, M. A. *Angew. Chem., Int. Ed.* **2000**, *39*, 2095. (e) Zhou, C.; Birney, D. M. *Org. Lett.* **2002**, *4*, 3279. (f) Caramella, P.; Quadrelli, P.; Toma, L. *J. Am. Chem. Soc.* **2002**, *124*, 1130. (g) Lasorne, B.; Dive, G.; Lauvergnat, D.; Desouter-Lecomte, M. *J. Chem. Phys.* **2003**, *118*, 5831. (h) Wales, D. J. *Energy Landscapes*, Cambridge University Press: Cambridge, New York, 2003. (i) Gonzalez-Lafont, A.; Moreno, M.; Lluch, J. M. *J. Am. Chem. Soc.* **2004**, *126*, 13089. (j) Suhrada, C. P.; Selçuki, C.; Nendel, M.; Cannizzaro, C.; Houk, K. N.; Rissing, P. J.; Baumann, D.; Hasselmann, D. *Angew. Chem., Int. Ed.* **2005**, *44*, 3548.

(31) Quapp, W.; Hirsch, M.; Imig, O.; Heidrich, D. *J. Comput. Chem.* **1998**, *19*, 1087.
(32) Quapp, W. *J. Chem. Phys.* **2005**, *122*, in press.
(33) The same type of analysis was performed on the reaction path of **4c** leading to qualitatively similar results.
(34) Williams, I. H.; Maggiora, G. M. *J. Mol. Struct.* **1982**, *6*, 365.

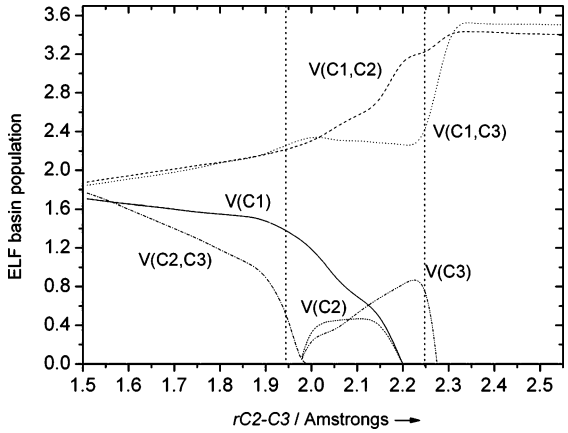

FIGURE 5. Integrated ELF basin populations for each point of the reaction path calculated by the rC2−C3 coordinate from **4t** to **5** (TS located at 2.03 Å). Vertical lines mark the change of the twisting motion (dis-/con-/disrotatory), as determined in Figure 4.

An analysis of the results presented in Figure 4 shows that the RC process can be dissected into three well-defined steps: (1) The first step happens in the range 1.53 Å (**4t**) ≤ rC2−C3 ≤ 1.95 Å, and the energy of the system (ΔE(step 1) = E(1.53) − E(1.95)) increases in 15.8 kcal/mol. The initial motion of the RC process occurs along a simultaneous and disrotatory (d1 = −d2) way. The most evident change in the electronic structure is associated with the weakening of the C2−C3 bond (V(C2,-C3) basin), transferring part of its charge to the C1−C2 and C1−C3 bonds (V(C1,C2) and V(C1,C3) basins) and, in a minor extent, to the C2−C11N and C3−C12N cyano groups. The lone pair containing the anion (represented by the V(C1) basin) does not participate in this part of the reaction and maintains a constant electron population, N[V(C1)] (see Figure 5). The ELF analysis yields less than 2.00e for N(V(C1)) because of a partial delocalization of the charge density through the cyano group C1−C10N. Thus, in agreement with one of the suggestions proposed by Breslow et al.,[3] the initial reaction path is associated with a disrotatory motion which is allowed by the WH rules because only the electron pair of the C2−C3 bond participates in this step. This behavior takes place until the C2−C3 bond-breaking process is almost completed (rC2−C3 = 1.90 Å). At the end of this step, both cyano groups (C2−CN and C3−CN) are nearly parallel (d1 = 100.0° and d2 = 80.0°); in terms of hybridization, the C2 and C3 carbons present a sp^2 character, whereas the C1 carbon keeps the initial sp^3 character. The d3 dihedral angle remains constant through this step to 117°. Finally, the C2−C3 bond breaking occurs for a rC2−C3 distance of 1.95 Å, as is shown in Figure 5 by the transformation of the V(C2,C3) disynaptic basin into the V(C2) and V(C3) monosynaptic ones. The presence of cyano groups on the C2 and C3 atoms enhances the process described along this step, lowering the energy barrier of the overall RC reaction. (2) The second step takes place in the range 1.95 Å < rC2−C3 < 2.25 Å, and the net change in energy, ΔE(step 2), is −3 kcal/mol. Figure 4 shows a change in the trend of d2, leading to a conrotatory-type process before the TS is reached (rC2−C3 = 2.03 Å). The ELF analysis shows that the lone pair represented by V(C1) commences to transfer electronic charge to the C1−C2 bond (see the increment N[V(C1,C2)] in Figure 5), and V(C2) moves toward V(C1,C2) to form a nearly double bond (reaching a population of 3.20e at the final stage of this step) between the C1 and C2 atoms. This process is facilitated by a planar arrangement of C1 and C2 atoms and their cyano substituents which corresponds to the continuous decrease of the d2 angle value (from 66.3° to 17.0°), whereas d1 also decreases but in a lower extension (from 89.3° to 73.6°) forming an allyl-radical-like species. The d3 angle changes smoothly along this step from 117° to 163°, according to the electronic changes reported. This result is consistent with de Lera et al.[5] findings of a conrotatory movement of cyano groups at the TS and its vicinities. (3) The last step occurs along the interval 2.25 Å < rC2−C3 ≥ 2.52 Å (**5**). The previous processes have lead to a situation of (nearly) double bonding between C1 and C2 atoms with a radical center at C3 (N[V(C3)] = 0.96e) being the anion that is delocalized through the cyano groups. A very large stabilization of the molecule can be obtained by planar delocalization of the allyl radical. Hence, a disrotatory movement of C2 and C3 cyano groups produced by the opening of the d1 angle (from 75.6° to 180°) and a small decrement of d2 lead to reach a planar conformation for the tricyano allyl system. Along this step, the system is largely stabilized, decreasing the energy (ΔE(step 3)) in 59.3 kcal/mol.

As we mentioned above, recently, de Lera et al.[5] showed in their computational study that the RC process of **4** starts out in the conrotatory fashion, changing to disrotatory after having passed the corresponding TS. However, the use of the IRC procedure, employed by these authors, presents serious drawbacks to representing the minimum energy path (from reactive to TS) due to the particular topology of the PES (see Figure 3). Our present study reveals new and more detailed information on the reaction mechanism: the reaction starts with the breaking of the C2−C3 bond via a disrotatory motion, followed by a shifting to conrotatory before the TS is reached and, finally, turning back to disrotatory because of the steric hindrance.

For comparison purposes, the same type of investigation was performed on reaction paths calculated for the 1-cyanocyclopropyl barrelene (**6**) and the unconstrained 1,2,3-tricyanocyclopropyl anion (**8**) (see Scheme 5), and the energetic results are summarized in Table 3. The process from **6** to **7** presents the same three-step mechanism separated by alternations of the twisting motion as given by the dihedral angles in the same way as **4t** (see Figure S1 of Supporting Information). However, the **TS1-III** is found for the rC2−C3 distance of 2.08 Å. The activation energy rises to 33.8 kcal/mol (15.5 kcal/mol higher than **4t**), and the reaction energy is exothermic in 26.2 kcal/mol (20.2 kcal/mol less than that for **4t**). Hence, the cyano groups at the C2 and C3 atoms in **4t** do not change the overall reaction mechanistic features of the PES, presenting the same type of steps as that of **6** but playing a decisive role in the stabilization of the relative energy of **TS1-I** and the allyl anionic product **5**. Analysis of the reaction path from **8** to **9** illustrates the effect of the geometrical constraint caused by the barrelene moiety (see Figure S2 in Supporting Information). The RC process of **8** presents an initial disrotatory motion practically identical to that for **4t**, also yielding a very similar energy barrier (17.5 kcal/mol at B3LYP/6-31+G(d)) and an earlier **TS1-IV** (rC2−C3 = 1.93 Å). The second step also presents the same type of conrotatory motion of the C2−CN and C3−CN groups, though the motion occurs in a faster and more simultaneous way (d1 and d2 run nearly parallel) than **4t**, leading directly to the planar product **9** along an exothermic reaction energy of 37.4 kcal/mol (B3LYP/6-31+G(d)). Therefore, the geometrical constraints imposed by the barrelene system on the RC of **4t**

SCHEME 4. Representation of ELF Basins along the RC Process[a]

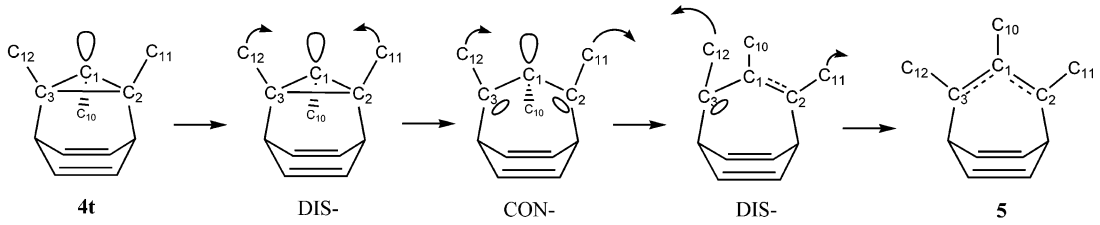

[a] The direction of movement of C2 and C3 cyano groups is indicated by the arrows. The solid line represents disynaptic basins (covalent bonds). Monosynaptic basins (electron pairs attached to one atom) are represented by ellipses. A dotted line indicates a largely populated basin.

SCHEME 5

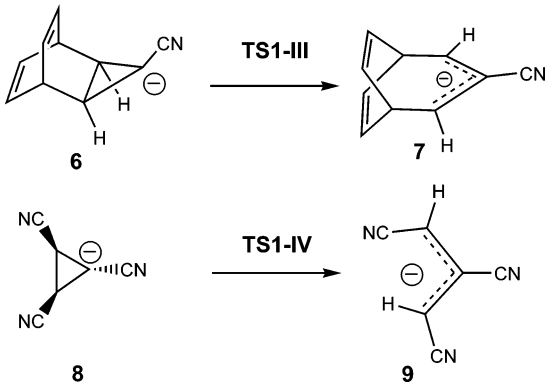

TABLE 3. Relative Energies (Δ*E* in kcal/mol) for the Stationary Points Involved in the Ring Cleavages of the Anions 6 and 8 to Yield 7 and 9

B3LYP/6-31+G(d)	
	Δ*E*
TS1-III	33.8
7	−26.2
TS1-IV	17.5
9	−37.4

[a] Relative to **6** or **8**, respectively.

do not modify the energy activation barrier but force the reaction mechanism toward a final disrotatory motion.

Finally, it is important to find an answer to the following question: why does only the anion **4** undergo the ring-cleavage process and not the neutral compound **3**? The picture derived from the present calculations points out that the reaction commences with the C2−C3 breaking process with concomitant electron-withdrawing effects of both cyano groups at C2 and C3. However, only for the anion **4**, it is possible that the electronic delocalization of the lone pair on C1 toward C1−C2 allows the stabilization of the diradicaloid system and reaches **TS1**−**I**. A further delocalization of the anion toward C1−C3 leads to the final allylic anion **5**, whereas the neutral system **3** cannot stabilize the diradicaloid resulting from C2−C3 bond breaking.

Conclusions

Theoretical calculations at the B3LYP/6-31+G(d), MP2/6-31+G(d), and G3(MP2) levels have been performed to study the two competitive mechanisms associated with the ring cleavage (RC) of the anionic cyclopropyl ring and the retrocycloaddition (rCA) reaction of the barrelene derivative **4c**−**t**. The present computational study enhances our understanding of the reactivity of the barrelene derivative and could stimulate experimental interest. In this work, examination of the potential energy surface of a RC reaction for **4t** gives clues as to what may be happening and novel arguments based on the analysis of the electron localization function (ELF) are presented to explain the unexpected process reported by Breslow et al.[3] A comparison with previous computational work by de Lera et al.[5] is also carried out. In summary, our theoretical results allow us to explain the experimental trends by means of these statements: (a) The RC process of the anion **4c**−**t** yields an allylic anion system via a concerted transition structure (**TS1-I**), whereas rCA is more energetically favorable along a two-stage mechanism, via two transition structures (**TS1-II** and **TS2-II**) and an intermediate (**IN-II**), than a concerted process via **TS3-II**. (b) The RC process is thermodynamically favored over the rCA reaction at the B3LYP/6-31+G(d), MP2/6-31+G(d), and G3(MP2) levels of theory. However, B3LYP predicts that RC and rCA reactions are kinetically competitive processes, whereas MP2 results point out that the RC process is the kinetically favorable process. There is an increasing divergence in terms of energies and geometries between the B3LYP and MP2 calculations as the rCA reaction progresses. An analysis based on isodesmic reactions points out the drawbacks of B3LYP in calculating bond dissociation energies associated with the carbon−carbon bond-breaking process along the present rCA reaction. (c) A detailed exploration of PES associated with the RC process allows us to characterize a valley-ridge inflection point in the uphill part. Therefore, we select the C2−C3 distance as an appropriate coordinate to analyze the progress of a RC reaction. This is due to the fact that the intrinsic reaction coordinate method is not a suitable approximation to analyze the reaction progress in this zone. (d) A complete analysis of the electronic rearrangements of the RC process by means of the ELF is carried out. The reaction mechanism can be described by three well-defined steps. (i) The initial C2−C3 bond-breaking process occurs via a disrotatory motion without participation of the lone pair on C1. The electron-withdrawing effect of cyano groups on the C2 and C3 atoms stabilizes the subsequent biradicaloid formation and lowers the activation energy barrier. (ii) Once the bond is broken (rC2−C3 = 1.95 Å), the lone pair on C1 is transferred to the C1−C2 bond via a conrotatory motion, forming an allyl-radical-like structure. The **TS1-I** is reached (rC2−C3 = 2.03 Å) at an early stage of this region. (iii) Finally, the anion is delocalized among the cyano groups and the allyl radical structure adopts a planar conformation via a disrotatory motion, forming a very stable product **5**. (e) Related systems (**6** and **8**) present common features with **4c**−**t**. An analysis and comparison of the results points out that the presence of cyano groups at the C2 and C3 atoms lowers the

activation energy barrier, and the constraint exerted by the barrelene unit on the overall reaction takes place in the downhill part of the PES, forcing the system to assume a final disrotatory motion. (f) A comparison of the RC process for the neutral, **3**, and anion **4** systems highlights the key role of the lone pair at the C1 of **4**. The stabilization of the system by delocalization of the anion after the C2−C3 bond-breaking process allows undergoing of the RC process through a low activation barrier. (g) The molecular mechanism of a given reaction can be analyzed along the reaction pathway by means of the evolution of the electron pairs derived from the ELF. This approach allows quantifying of the relationship between the bond-breaking/-forming processes and the rearrangements of the electronic density among the electron pairs by means of flows of electronic charge, allowing a sound rationalization of geometric and energetic changes along the reaction path connecting the reactants to the products.

Acknowledgment. This work was supported by the Universitat Jaume I-Fundacio Bancaixa, Project P1B99-02, Ministerio de Ciencia y Tecnología, DGICYT, Projects BQU2002-01032 and BQU2003-04168-C03-03, and Generalitat Valenciana, Projects GRUPOS02-028 and GRUPOS03/176. The authors thank Prof. R. Breslow for the fruitful comments on the manuscript. The authors also acknowledge the Servei d'Informatica, Universitat Jaume I, for a generous allotment of computer time.

Supporting Information Available: Full citation for ref 13. Figures S1 and S2. List of B3LYP/6-31+G(d) optimized Cartesian coordinates and energies (in Å and atomic units, respectively) for all species involved in the discussion. This material is available free of charge via the Internet at http://pubs.acs.org.

JO052117H